Electronic Supplementary Information: Controlling the structures of organic semiconductor - quantum dot nanocomposites through ligand shell chemistry

Daniel T. W. Toolan*[1], Michael P. Weir*[2], Rachel C. Kilbride[2], Jon R. Willmott[3], Stephen M. King[4], James Xiao[5], Neil C. Greenham[5], Richard H. Friend[5], Akshay Rao[5], Richard A. L. Jones[2] and Anthony J. Ryan[1]

1. *Department of Chemistry, The University of Sheffield, Dainton Building, Brook Hill, Sheffield, S3 7HF, UK*
2. *Department of Physics and Astronomy, The University of Sheffield, Hicks Building, Hounsfield Road, Sheffield, S3 7RH, UK*
3. *Department of Electronic and Electrical Engineering, The University of Sheffield, 3 Solly Street, Sheffield, S1 4DE, UK*
4. *ISIS Pulsed Neutron and Muon Source, STFC Rutherford Appleton Laboratory, Didcot, OX11 0QX, UK*
5. *Cavendish Laboratory, Cambridge University, J. J. Thomson Avenue, Cambridge, CB3 0HE, UK*

*Authors to whom correspondence should be addressed. These authors contributed equally to this work.
DTWT: d.toolan@sheffield.ac.uk, MPW: weir.mp@gmail.com

Table of contents

1. Spectroscopic characterisation of QD

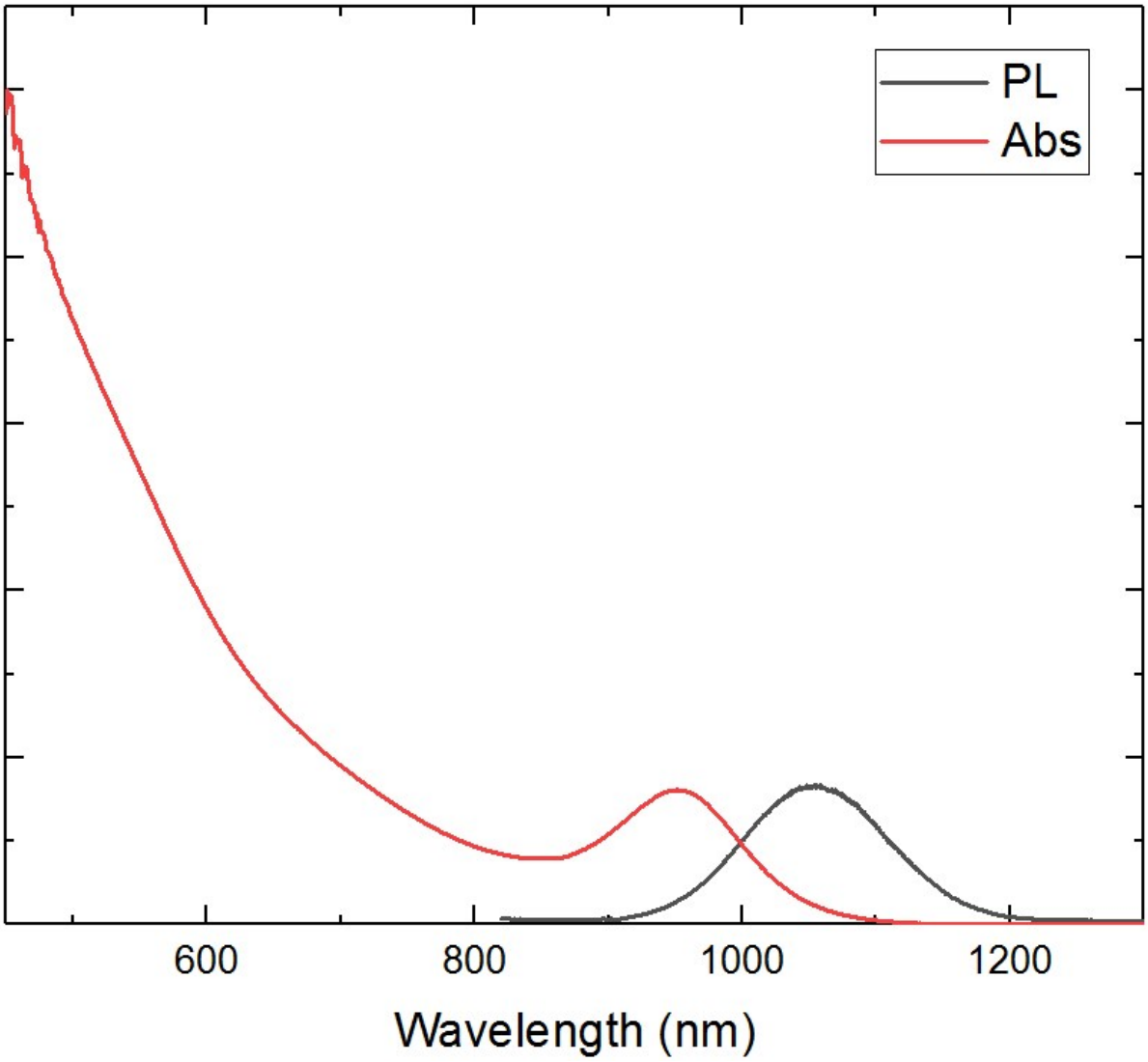

Supplementary Figure S1. Absorption (red) and photoluminescence (grey) spectra of as-synthesised PbS-OA QDs.

2. Small-angle scattering models

2.1. Sphere model

In small-angle X-ray scattering (SAXS) of PbS nanocrystals suspended in an organic solvent such as toluene, the (organic) ligand shell and solvent are effectively contrast-matched and therefore scattering is dominated by the high electron density, metal-rich core. As PbS cores are quasi-spherical, they are adequately modelled as spherical scattering particles. The form factor of such particles, expressed as the scattering intensity as a function of the magnitude of the scattering vector, q, is given by

$$I(q) = \frac{scale}{V}\left[3V(\Delta\rho)\frac{\sin(qr) - qr\cos(qr)}{(qr)^3}\right]^2 + background$$

where r and V are the radius and volume of the sphere, $\Delta\rho$ is the scattering length density contrast difference between the solvent and the spherical particle. For data that has been correctly normalised onto an absolute intensity scale in units of cm^{-1} (i.e. at the experimental and initial data reduction stages, described in the *Experimental* section of the main manuscript under the sub-headings *Small-angle neutron scattering* and *Small-angle X-ray scattering*) the $scale$ represents the volume fraction of scattering particles.

2.2. Core-shell sphere model

In small-angle neutron scattering (SANS) of PbS nanocrystals suspended in an organic solvent, the organic ligand shell may contribute significantly to the measured scattering, particularly if it has been highlighted by manipulating the neutron contrast (in the case of manuscript Figure 1, using deuterated toluene). The core-shell sphere model takes the scattering from the shell into account and is a development of the sphere model. Terms are included to account for scattering both from the core and from the additional shell, so that the form factor is given by

$$I(q) = \frac{scale}{V}F^2(q)$$

where

$$F(q) = 3\left[V_c(\rho_c - \rho_s)\frac{\sin(qr_c) - qr_c\cos(qr_c)}{(qr_c)^3} + V_s(\rho_s - \rho_{solv})\frac{\sin(qr_s) - qr_s\cos(qr_s)}{(qr_s)^3}\right]^2$$

where, V_c and V_s are the volumes, r_c and r_s are the radii, and ρ_c and ρ_s are the scattering length densities of the core and shell respectively, and ρ_{solv} is the scattering length density of the solvent. This model has been useful to describe the ligand shell structure in as-synthesised lead sulfide-oleic acid quantum dots[1]. In the current study it is used to ascertain the thickness and composition of ligand shells post-exchange.

2.3. Structure factors

The expressions for $I(q)$ above are for isolated scattering objects, and are known as form factors since they describe the scattering features that emerge from the object's intrinsic shape and form alone. However, in a many-particle system like a solution or nanocomposite of colloidal quantum dots, scattering may also arise from inter-particle correlations. This scattering is taken into account by a *structure factor* $S(q)$ that multiplies the form factor at each point in q, i.e.

$$I(q) = F(q)S(q)$$

For relatively low concentrations typical of high-contrast experiments such as a solution SAXS experiment on PbS colloidal quantum dots in an organic solvent, say 1-10 mg mL^{-1}, [e.g. manuscript Figure 1(a)] the structure factor is a minor perturbation, such that it barely makes a visible adjustment to the data. If the system is sufficiently dilute it may be possible not to use the structure factor at all. For relatively high concentrations typical of low-contrast experiments such as the analogous SANS experiment using (for example) a deuterated solvent, say 10-100 mg mL^{-1}, the structure factor is a significant feature of $I(q)$ and must be taken into account using the appropriate function. In concentrated systems the structure factor may begin to dominate the form factor such that correlations from inter-particle interactions are of primary importance in describing the observed scattering features.

2.3.1. Hard sphere structure factor

The hard sphere structure factor (as implemented in SasView version 4.2.2) is a calculation of the interparticle structure factor for monodisperse spherical particles interacting through excluded volume interactions. This is calculated using the Percus-Yevick closure[2] where the inter-particle potential is given as:

$$U(r) = \begin{cases} \infty & r < 2R \\ 0 & r \geq 2R \end{cases}$$

2.3.2. Sticky hard sphere structure factor

The sticky hard sphere structure factor (as implemented in SasView version 4.2.2) is a calculation of the interparticle structure factor for monodisperse spherical particles interacting via a narrow, attractive, potential well. This is calculated using a

perturbative solution to the Percus-Yevick closure[3,4]. The inter-particle potential is given by

$$U(r) = \begin{cases} \infty & r < \sigma \\ -U_0 & \sigma \leq r < \sigma + \Delta \\ 0 & r > \sigma + \Delta \end{cases}$$

where the stickiness parameter quantifying the attractiveness of the well is given by

$$\epsilon = \frac{1}{12\tau}\exp\left(U_0/k_B T\right)$$

where U_0 is the depth of the potential well. The stickiness ϵ is also dependent upon the perturbation parameter τ, which sets the width of the well via the relation $\tau = \Delta/(\sigma + \Delta)$. Here, σ is the classical hard sphere radius of $2R$ and Δ is the width of the potential well.

2.4. Size polydispersity in quantum dots

2.4.1. Gaussian distribution

The Gaussian distribution as implemented in SasView 4.2.2[5] was applied to represent the polydispersity in the thickness of quantum dot ligand shells pre- or post-exchange.

$$f(x) = \frac{1}{Norm}\exp\left(-\frac{(x-\bar{x})^2}{2\sigma^2}\right)$$

In this notation, x represents the ligand shell thickness, $Norm$ is the normalisation factor, $\bar{x}$ is the mean ligand shell thickness, and σ describes the width of the distribution. It is related to the polydispersity value via the relation $PD = \sigma/\bar{x}$ such that a typically obtained value of a mean thickness of $\bar{x}$ = 15 Å with PD = 0.1 with relates to a Gaussian width of 1.5 Å.

2.4.2. Lognormal distribution

The lognormal distribution as implemented in SasView 4.2.2[5] was used to describe the polydispersity in the radii of quasi-spherical PbS quantum dot cores. It is usually obtained from a SAXS measurement (see manuscript Figure 1(a)) which provides the optimal contrast. The lognormal distribution is a function of r for which $\ln r$ has a normal distribution.

$$f(r) = \frac{1}{Norm}\frac{1}{r\sigma}\exp\left(-\frac{1}{2}\left(\frac{\ln r - \mu}{\sigma}\right)^2\right)$$

In this notation, r represents the radius of the quasi-spherical quantum dot core, $Norm$ is the normalisation factor, $\mu = \ln r_{med}$ and r_{med} is the median value of the lognormal distribution and σ describes the width of the underlying normal distribution.

3. FOXS fit to small-angle neutron scattering data

3.1. Details of the FOXS calculation

Briefly, the chemical structure (3D conformer) of TIPS-Tc was obtained in .sdf format from PubChem[6] (U.S. National Library of Medicine) and converted into a Protein Data Bank (.pbd) format using OpenBabel. The FOXS server was then used to calculate the small-angle X-ray scattering pattern that would be expected from the molecule in H_2O. The .pdb file was used as the "Input molecule" and the 25 mg/mL SANS data was used as a dataset to fit with the SAXS profile ("Experimental profile"). Using the Advanced Options, the following processing parameters were selected, which are the default choices unless specified: a maximal *q* value of 0.99 Å^{-1} (non-default, to capture the full range of features measured in the SANS profile) a profile size of 500 points, a hydration layer, excluded volume adjustment, implicit hydrogens, and an offset (non-default, to take into account the differences in contrast in comparing SANS in d-toluene to SAXS in H_2O). The resulting profile (SAXS model fit to the SANS data) are presented in Figure 2 of the main manuscript.

3.2. Comparison with simpler models

3.2.1. Guinier

A simple Guinier fit follows the expression

$$I(q) = scale \times \exp\left(\frac{-qR_g{}^2}{3}\right) + background$$

and is used in order to capture the radius of gyration R_g representing the distribution of an object's scattering length density around its centre of mass. It therefore represents one of the simplest possible models of the solution structure of dilute TIPS-Tc. Using the full data range from the SANS from TIPS-Tc at 25 mg/mL in d-toluene (solvent subtracted), it is not adequate to capture the inflection in $I(q)$ at *q* = 0.4 Å^{-1}.

However, it captures the overall size of TIPS-tetracene by using a restricted *q*-range with q_{max} = 0.34 Å^{-1}, i.e. fitting only the low-*q* region representing the object's overall size (but maintaining a physical constraint on the background of a maximum of 0.015 cm^{-1}), yielding a radius of gyration of 6.6 ± 0.3 Å.

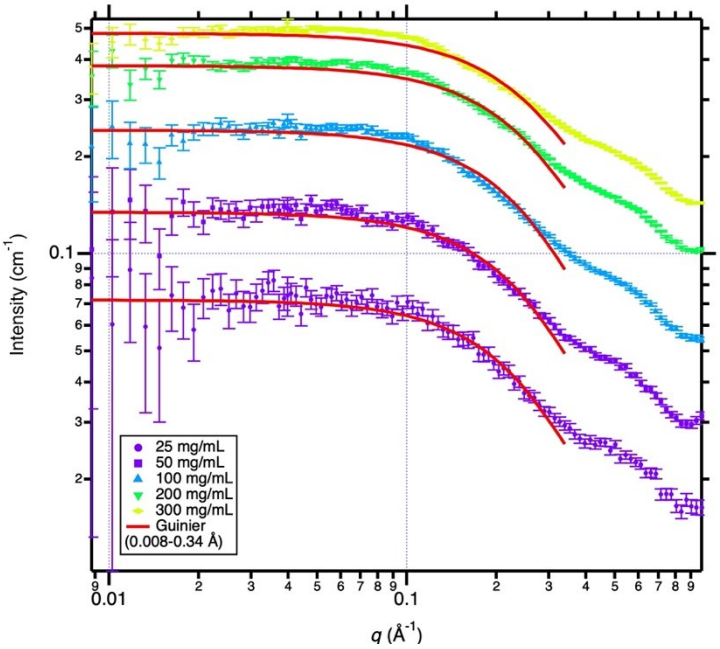

Supplementary Figure S2. Guinier fits to SANS data for TIPS-Tc in d-toluene (solvent subtracted) at 25, 50, 100, 200 and 300 mg/mL using a q-range of 0.008-0.34 Å^{-1} to capture the overall size of the scattering objects

3.2.2. **Ellipsoid**

The ellipsoid model as implemented in SasView 4.2.2[7] calculates the scattering from an ellipsoidal object characterised by a polar radius and an equatorial radius (including possible polydispersity independently in either). The object and surrounding solvent have spatially uniform scattering length densities. Assuming that the anisotropic shape of TIPS-Tc cannot be fitted using any model with spherical symmetry, an ellipsoid was suggested as a candidate for the next simplest alternative model. Given that the approximate [diametric] dimensions a) along the tetracene moiety and b) from TIPS-TIPS are ~ 10 Å and ~ 14 Å respectively, the initial guesses for the polar and equatorial radii were set at 5 Å and 7 Å respectively. Having no *a priori* knowledge of the appropriate ellipsoid representing TIPS-Tc, the ellipsoid radii were allowed to vary from 2.5 – 14 Å, i.e. from half of the shorter dimension to twice the of the longer dimension. Scattering length densities were fixed at $\rho_{TIPS-Tc}$ = 1.1 × 10^{-6} Å^{-2} $\rho_{d-toluene}$ = 5.68 × 10^{-6} Å^{-2} and the background was constrained to a maximum value of 0.015 cm^{-1}. Nominal polydispersites of 0.05 were ascribed to the ellipsoid radii but no limits

were placed on them during fitting. In short, the ellipsoid model was able to produce a fair fit of the Guinier region but failed to reproduce the inflection at q = 0.4 Å^{-1}.

4. QD with TIPS-Tc concentration series

4.1. Additional SANS data

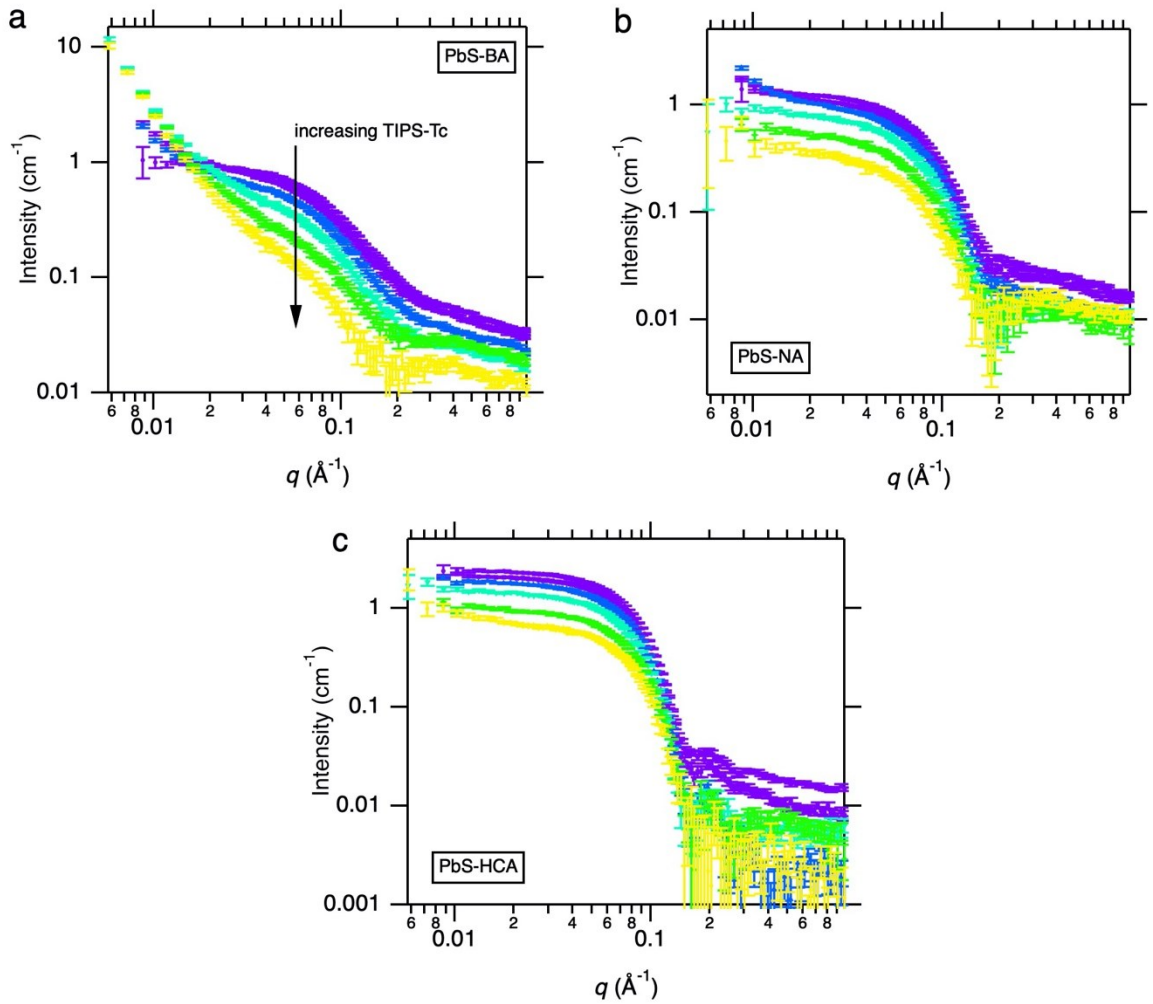

Supplementary Figure S3. SANS data for (a) PbS-BA, (b) PbS-NA and (c) PbS-HCA as TIPS-Tc is sequentially added at 0, 25, 50, 100, 200 and 300 mg/mL, with the appropriate TIPS-Tc background subtracted from each curve.

concentrations of 25, 50, 100, 200 and 300 mg/mL. In each case, the appropriate TIPS-Tc background has been subtracted. Figure S3 extends this to show the data for PbS-NA and PbS-HCA. Starting with the SANS curve from the exchanged QDs in d-toluene ("zero" TIPS-Tc), the scattering from the PbS(-BA, -HCA & -NA) with the full range of TIPS-Tc concentrations is presented. In each case, the addition of TIPS-Tc appears to promote QD aggregation, with a notable decrease in the scale of the core-

shell-sphere form factor (indicative of fewer isolated QDs) and an upturn in scattering at low *q* indicative of scattering from QD aggregates, which is particularly prominent for the PbS-BA:TIPS-Tc solutions.

4.2. Mass fractal model: for scale factor only

The data range available in the current study was insufficient to make a determination the mass fractal nature of the quantum dot aggregates formed. Here, we present a short treatment of the data with a mass fractal model from the perspective of extracting some scale factor using the model only as an illustration over a limited sub-range. The mass fractal model utilised to fit the data is implemented in SasView. It begins with a form factor for spherical scattering particles and calculates the scattering from a fractal aggregate of the particles following the formalism of Mildner and Hall[8]. The model calculates a structure factor to describe the aggregation of spherical subunits of radius R into mass fractal structures. For this model, $I(q)$ is calculated as

$$I(q) = scale \times P(q)S(q) + background$$

Here, $P(q) = F(qR)^2$ where

$$F(x) = \frac{\sin(x) - x\cos(x)}{x^3}$$

is an element of the spherical particle form factor (ESI section 2.1). The main substance of the model is the structure factor given by

$$S(q) = \frac{\Gamma(D_m - 1)\zeta^{D_m - 1}\ \sin\left[(D_m - 1)\tan^{-1}(q\zeta)\right]}{\left[1 + (q\zeta)^2\right]^{(D_m - 1)/2}} \qquad q$$

where ζ is the correlation or cut-off length representing the maximum size of mass fractal aggregates, D_m is the mass fractal dimension, ranging from 1 to 6, and $\Gamma(z) = \int_0^\infty x^{z-1}e^{-x}dx$. For data that is correctly normalised into absolute units of cm^{-1}, $scale = NV^2\left(\rho_p{}^2 - \rho_s{}^2\right)$

where ρ_p and ρ_s are the neutron scattering length densities of the particle and solvent respectively, and the volume of the spherical nanoparticle is $V = \frac{4}{3}\pi R^3$. The scale factor therefore allows an estimation of the number of quantum dots included in aggregates for absolutely calibrated data.

The form-factor-subtracted sample data, for all PbS-BA samples (25 to 300 mg/mL TIPS-Tc) and for PbS-NA and PbS-HCA at 300 mg/mL TIPS-Tc, were fitted to a mass fractal model with a severely limited range of 0.01 – 0.4 Å^{-1} to provide insight into the scale factor only. This was done using a sub-unit radius of 16 Å (i.e. assuming that the scattering subunit is similar in size to a PbS QD) and an arbitrarily large cut-off length of 100000 Å to indicate that the full size of the aggregates is much larger than the SANS measurement window. The current SANS data range suggests a minimum in the mass fractal correlation length, i.e. a minimum cluster size, of 300 Å. The PbS-NA:TIPS-Tc and PbS-HCA:TIPS-Tc (300 mg/mL) samples both exhibit similar aggregation type features, albeit with a much lower volume fraction of QD aggregates. The scale factor, proportional to the total number of scatterers in the mass fractal[8] was observed using a fixed exponent of -2.5 (to ensure a level comparison between datasets) showing that for the PbS-BA:TIPS-Tc concentration series, the number of scatterers plateaus at 100 mg/mL TIPS-Tc. For all the QDs at 300 mg/ml TIPS-Tc, PbS-NA and PbS-HCA are found to produce about 0.07 and 0.09 times the volume (number of scatterers) of mass fractals than PbS-BA (see Figure S4).

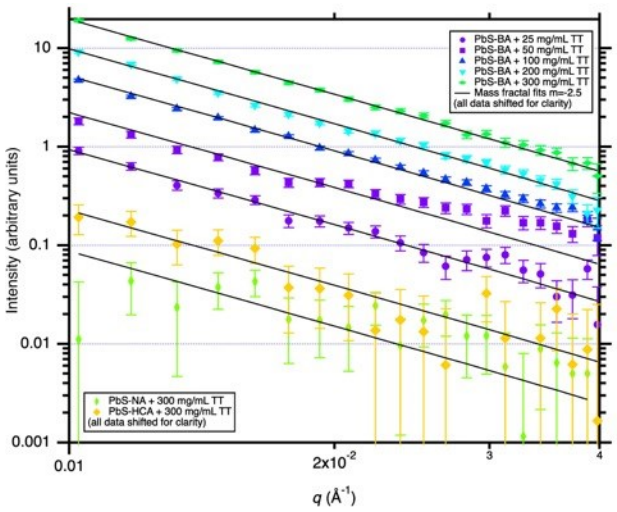

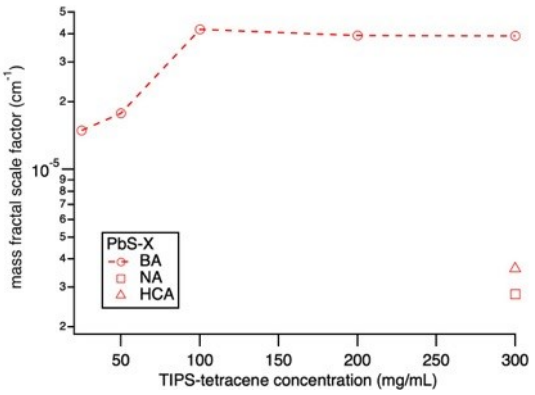

Supplementary Figure S4. (a) Fixed m=-2.5 mass fractal fits to the "power law only" data for PbS-BA 25-300 mg/mL and PbS-NA and PbS-HCA 300 mg/mL, with data scaled for clarity. (b) scale factors obtained from the fits in part (a) to provide estimates of the relative total numbers of scatterers in a mass fractal arrangement for each different sample.

5. SAXS on extracted supernatant solutions

SAXS was performed on the extracted supernatant solutions and compared to the original SANS data in order to gain insight into changes in QD structure that may have occurred as a consequence of the crystallization process (with data shown, Figure S5). Data for all supernatants (PbS-BA, PbS-HCA, PbS-NA, with TIPS-Tc) do not show any evidence of TIPS-Tc crystallites in solution, with the predominant scattering features arising from the highly electron dense PbS QD cores. For PbS-BA (Figure. S5(a)), the supernatant was compared to the original scattering from PbS-BA in d-toluene as measured using SANS by performing a co-refinement of both datasets using the core-shell-sphere + Guinier model. A satisfactory fit was obtained for both datasets by fixing the core radius, the shell thickness and polydispersity, and the Guinier radius of gyration. The cases of PbS-NA and PbS-HCA were relatively straightforward because the supernatant data were well fitted by *sphere*hard sphere* models (with modest improvements available by using a *core-shell-sphere*hard sphere* model, despite the poor contrast between organic ligands and solvent). It was therefore possible to conclude that all three supernatants retained from TIPS-Tc/QD composite crystals comprised isolate QD with similar structures to their initial QD solutions.

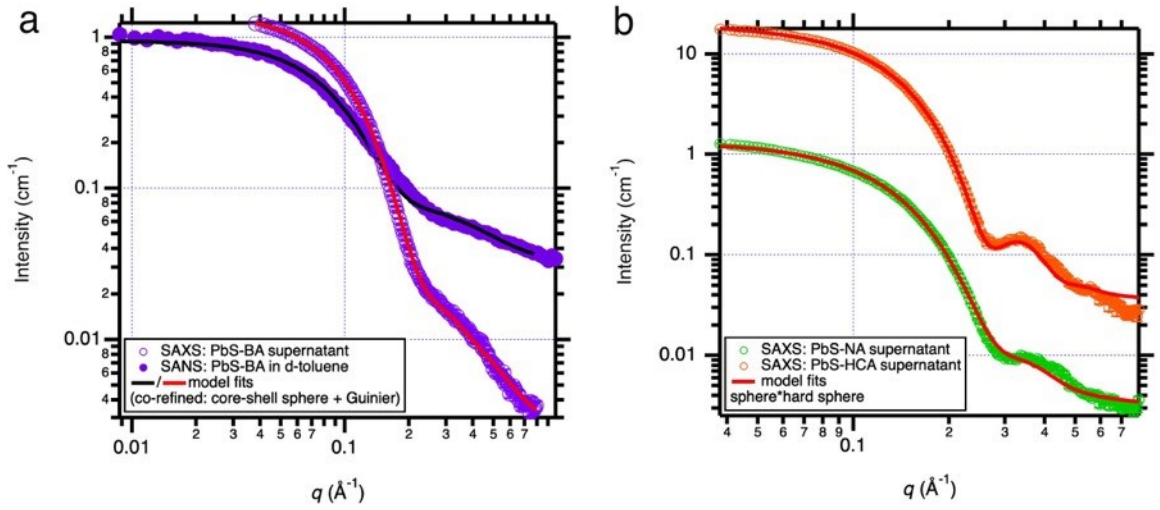

*Supplementary Figure S5. Small-angle scattering measurements of the supernatants separated from TIPS-Tc/QD composite crystals. (a) Comparison of the PbS-BA supernatant with the original PbS-BA SANS data. Co-refined SAXS and SANS using a core-shell sphere plus Guinier model, indicating no significant structural changes in the supernatant compared with the to the initial QD in solution. (b) SAXS fitting using a sphere*hard sphere model to the supernatants of PbS-NA and PbS-HCA, indicating isolated QD without significant aggregation.*

6. Wide-angle X-ray scattering on crystals

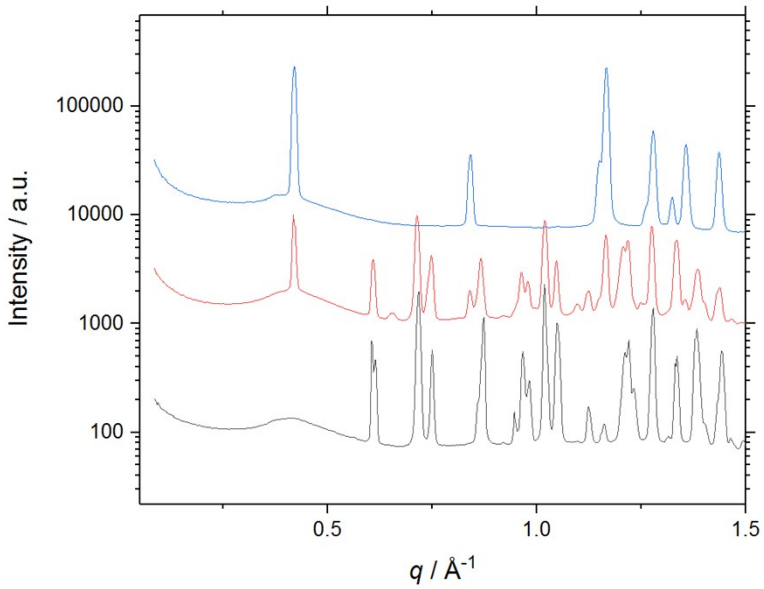

Supplementary Figure S6. Wide angle x-ray scattering measurements of NA (blue), NA:TIPS-Tc (red) and TIPS-Tc (black) crystals formed via evaporation of solvent.

7. Supplementary data on DMF annealing

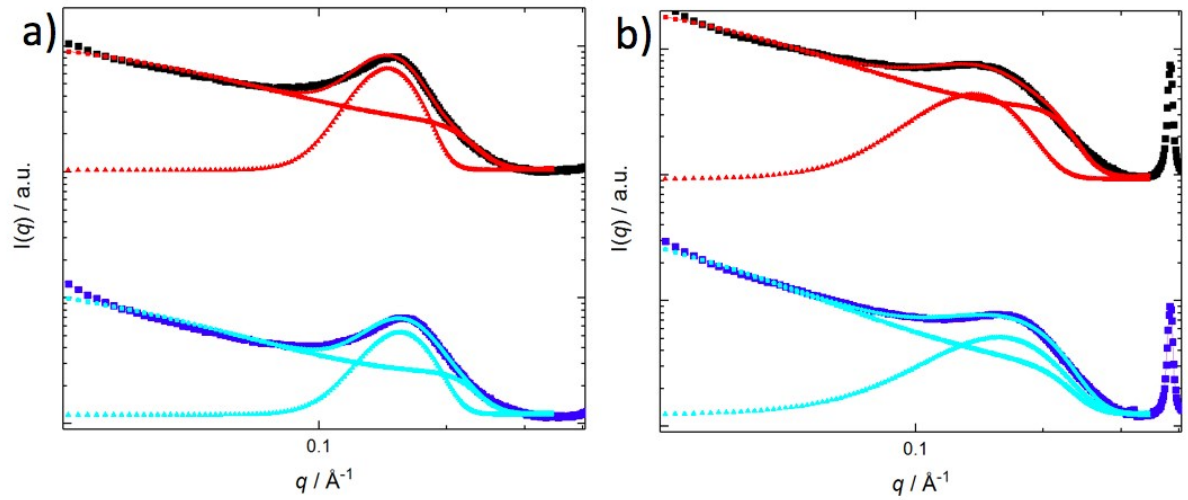

*Supplementary Figure S7. Small-angle scattering measurements of the a) PbS-HCA:TIPS-Tc and b) PbS-NA:TIPS-Tc composite crystals, pre- (black line) and post- (dark blue line) DMF solvent anneal. Showing model fits sphere*sticky hard sphere + Gaussian peak (circles) and constituent components of model, sphere*sticky hard sphere (squares) and Gaussian peak (triangles).*

8. References

1 Weir, M. P. *et al.* Ligand Shell Structure in Lead Sulfide–Oleic Acid Colloidal Quantum Dots Revealed by Small-Angle Scattering. *The Journal of Physical Chemistry Letters* **10**, 4713-4719, doi:10.1021/acs.jpclett.9b01008 (2019).

2 Percus, J. K. & Yevick, G. J. Analysis of Classical Statistical Mechanics by Means of Collective Coordinates. *The Physical Review* **110**, 1 (1958).

3 Menon, S. V. G., Manohar, C. & Rao, K. S. A new interpretation of the sticky hard sphere model. *The Journal of Chemical Physics* **95**, 9186, doi:1.461199 (1991).

4 Baxter, R. J. Percus–Yevick Equation for Hard Spheres with Surface Adhesion. *The Journal of Chemical Physics* **49**, 2770, doi:1.1670482 (1968).

5 SasView 4.2.2. user documentation. http://www.sasview.org/docs/old_docs/docs_4.2.2/user/sasgui/perspectives/fitting/pd/polydispersity.html (accessed 3rd June 2020.)

6 *National Center for Biotechnology Information. PubChem Database. CID=58870962, https://pubchem.ncbi.nlm.nih.gov/compound/5_12-Bis__triisopropylsilyl_ethynyl_tetracene (accessed on Oct. 22, 2019).*

7 SasView 4.2.2. user documentation. http://www.sasview.org/docs/old_docs/docs_4.2.2/user/models/ellipsoid.html (accessed 3rd June 2020).

8 Mildner, D. F. R. & Hall, P. L. Small-angle scattering from porous solids with fractal geometry. *Journal of Physics D: Applied Physics* **19**, 1535-1545 (1986).